Global Change Biology

Global Change Biology (2014) **20**, 581–593, doi: 10.1111/gcb.12393

Drought footprint on European ecosystems between 1999 and 2010 assessed by remotely sensed vegetation phenology and productivity

EVA IVITS*, STEPHANIE HORION†, RASMUS FENSHOLT† and MICHAEL CHERLET*

*DG Joint Research Centre, Institute for Environment and Sustainability, Land Resource Management Unit, TP 280, Via E. Fermi, 2749 Ispra, VA I-21027, Italy, †Department of Geosciences and Natural Resource Management (IGN), University of Copenhagen, Oester Volgade 10, Copenhagen K 1350, Denmark

Abstract

Drought affects more people than any other natural disaster but there is little understanding of how ecosystems react to droughts. This study jointly analyzed spatio-temporal changes of drought patterns with vegetation phenology and productivity changes between 1999 and 2010 in major European bioclimatic zones. The Standardized Precipitation and Evapotranspiration Index (SPEI) was used as drought indicator whereas changes in growing season length and vegetation productivity were assessed using remote sensing time-series of Normalized Difference Vegetation Index (NDVI). Drought spatio-temporal variability was analyzed using a Principal Component Analysis, leading to the identification of four major drought events between 1999 and 2010 in Europe. Correspondence Analysis showed that at the continental scale the productivity and phenology reacted differently to the identified drought events depending on ecosystem and land cover. Northern and Mediterranean ecosystems proved to be more resilient to droughts in terms of vegetation phenology and productivity developments. Western Atlantic regions and Eastern Europe showed strong agglomerations of decreased productivity and shorter vegetation growing season length, indicating that these ecosystems did not buffer the effects of drought well. In a climate change perspective, increase in drought frequency or intensity may result in larger impacts over these ecosystems, thus management and adaptation strategies should be strengthened in these areas of concerns.

Keywords: drought, ecosystems, Europe, PCA, phenology, productivity

Received 16 November 2012 and accepted 31 August 2013

Introduction

Drought affects more people than any other natural disaster and is considered to be one of the most costly natural hazards (Wilhite, 2000). Between 1999 and 2010, over 900 million people worldwide have been affected by drought (EMDAT, 2011). According to Dai *et al.* (2004) the geographic area affected by drought has strongly increased globally over the last four decades. However, using improved evapotranspiration models, recent findings of Sheffield *et al.* (2012) plead for little evidence of increase in the total area affected by drought over the past 60 years. These authors pointed out the high uncertainties in global-scale drought trends as a result of methodological limitations of temperature-based models used to estimate the contribution of evapotranspiration as driver for droughts (Seneviratne, 2012; Sheffield *et al.*, 2012). Nevertheless, in the last decades notable droughts were registered in diverse parts of the world triggering crop failures, increased pressure on the stock markets, and eventually casualties due to famine in food-insecure regions and/or harmful health conditions (Horion *et al.*, 2012). An increase in the frequency and duration of drought events might contribute to global warming through positive carbon-climate feedback mechanisms if temperate ecosystems are turned from carbon sinks to carbon sources (Ciais *et al.*, 2005) and might contribute to the irreversible degradation of ecosystems (Anderegg *et al.*, 2013). The monitoring of negative effects of drought is therefore of outmost importance and requires an identification of the factors influencing the vulnerability of a region to dry spells (Wilhite, 2002) and thorough understanding of ecosystem response to drought (van der Molen *et al.*, 2011).

Timely information about the onset of drought, its extent, intensity and duration can limit drought-related losses of life, reduce pressure on food-insecure regions and on the environment in general (Brown & Funk, 2008; Horion *et al.*, 2012). Traditional methods of drought monitoring are based on meteorological indices derived from weather station data (Landsberg,

Correspondence: Eva Ivits, DG Joint Research Centre, TP 280, Via E. Fermi, 2749, Ispra (VA) I-21027, Italy, tel. +39-0332-785315, e-mail: eva.ivits-wasser@ext.jrc.ec.europa.eu

1986; WMO, 2006). The Standardized Precipitation Index (SPI, McKee *et al.*, 1993) and the Palmer Drought Severity Index (PDSI, Palmer, 1965) are two of the most commonly used indicators for operational drought monitoring. Both indicators have been demonstrated to be useful for meteorological, agricultural, and hydrological drought in multiple studies (e.g. Bordi & Sutera, 2001; Mishra & Singh, 2010). The Standardized Precipitation and Evapotranspiration Index (SPEI) is an enhanced data set showing improved capabilities to identify drought impacts as compared with standard drought indicators, such as the PDSI or the SPI (Vicente-Serrano *et al.*, 2010). In the last decades, Earth Observation (EO) data have also gained more attention for timely drought detection and impact assessment on vegetation productivity (e.g. Ji & Peters, 2003; Ciais *et al.*, 2005; Vicente-Serrano, 2007; Gouveia *et al.*, 2009; Udelhoven *et al.*, 2009; Fensholt *et al.*, 2010; Rhee *et al.*, 2010; Caccamo *et al.*, 2011).

Regional to subcontinental scale impact of drought on vegetation cover and the severity of damage remain a pivotal uncertainty in projected climate change conditions (Rustad *et al.*, 2001; Breshears *et al.*, 2005; Seneviratne 2012). There are still uncertainties in how species competitions and ecosystems composition respond to drought (Walther *et al.*, 2002; van der Molen *et al.*, 2011) and the response of plant productivity to climate change is variable with various effects reported (Rustad *et al.*, 2001). The same precipitation deficit will affect two regions differently as a function of the specific (bioclimatic, edaphic, etc.) conditions of each region. Similarly, drought impacts will vary depending on the timing of the drought occurrence in relation to species distribution within the region/ecosystem and the respective phenology and capacity to cope with drought-induced stress. Furthermore, key-environmental factors such as soil moisture conditions prior to drought events and anomalously high temperatures also trigger different vegetation responses (Breshears *et al.*, 2005). Indeed, variable plant responses were already shown to warming and drought in an experimental North-South European gradient depending on site locations, seasons, and species (Peñuelas *et al.*, 2004). Providing an accurate assessment of vegetation response to drought-induced stress at continental or global scale remains challenging despite the substantial number of EO derived indices potentially useful to analyze impacts (Bordi *et al.*, 2009; Zhao & Running, 2010; Medlyn, 2011; van der Molen *et al.*, 2011; Samanta *et al.*, 2011).

Southern and central Europe has been reported to experience more intense and longer droughts since the 1950's (Van der Schrier *et al.*, 2006; Vicente-Serrano, 2007; Gouveia *et al.*, 2009; Udelhoven *et al.*, 2009; Lindner *et al.*, 2010; Dai, 2011; Sousa *et al.*, 2011). However, reports of drought impacts in other parts of Europe are comparably scarce. In this study, we focus on the assessment of drought impact – or footprint – on the vegetation productivity and phenology of all European ecosystems by jointly analyzing spatio-temporal patterns of drought conditions with vegetation phenology and productivity changes between 1999 and 2010. Drought conditions were evaluated by the SPEI whereas the spatio-temporal pattern in the 12 year period was assessed by a Principal Component Analysis (PCA). Vegetation productivity and phenology of the ecosystems were assessed by decomposing satellite observed time-series of SPOT VEGETATION Normalized Difference Vegetation Index (NDVI) into yearly estimates of vegetation productivity and growing season length (SL). The research aim is twofold: (i) to understand if the observed spatio-temporal pattern of drought co-occurred with changes in vegetation productivity and phenology between 1999 and 2010 and (ii) to evaluate if differences in ecosystem responses and resilience could be identified at the continental scale as a function of land cover classes and different bioclimatic conditions.

Materials and methods

Drought dataset

The gridded global drought dataset SPEI (dataset v2.0) was used in the current study (Vicente-Serrano *et al.*, 2010). Besides the input from precipitation, SPEI also accounts for the possible effects of temperature variability and temperature extremes by implying data on evapotranspiration. The FAO-56 Penman-Monteith's method (Allen *et al.*, 1998) has been used for computing PET and the dataset of gridded precipitation and temperature at the global scale used for the SPEI was acquired from Climatic Research Unit (CRU) TS (time-series) data set. Monthly SPEI data covering the time scale of 12 months (SPEI12) from 1999 to 2010 at a spatial resolution of 0.5° lat/long was used. A timescale of 12 months (or longer) is commonly used to monitor long-lasting dry episodes and therefore consequently is more sensible to detect hydrological drought compared with shorter timescales that instead target the detection of meteorological and/or agricultural droughts (Bordi & Sutera, 2001). Vicente-Serrano (2006) showed that vegetation activity during the germination period in cereals, shrubs, and pastures is mainly determined by the precipitation accumulated over the previous 12 months. Also Wang *et al.* (2003) have indicated that the dry-farming and pasture productions on the Great Plains of the USA are not only determined by the precipitation recorded during the year but also by the precipitation that fell in the previous year. These authors indicated that initial levels of soil moisture at the beginning of the growing season are best summarized by means of a wide time scale for the drought index (Vicente-Serrano, 2006).

Vegetation phenology and productivity datasets

Normalized Difference Vegetation Index data at a spatial resolution of 1 × 1 km and a temporal resolution of 10 days were acquired from the SPOT VEGETATION sensor produced and distributed by VITO (http://free.vgt.vito.be/). The time span of the data covered 1 January 1999 to 31 December 2010. Yearly values of SL and an approximation of Net Primary Productivity (NPP) were derived from the NDVI time-series using the algorithm of the 'Phenolo' package developed at the EC Joint Research Centre (Ivits *et al.*, 2012a). The preprocessing of the NDVI time-series (missing value handling, interpolation to daily values, and smoothing to remove short peaks and drop-offs) results in a 'reference time-series' on which the phenological parameters were computed by intersecting this preprocessed time-series with lagged moving averages (MA, see Fig. 1a). Phenolo includes an automated per-pixel adjustment, where the lag for the MA algorithm is computed using the temporal dynamics of each pixel. The lag is derived from the yearly phenological dynamics of the pixels and subsequently these yearly values are averaged along the time series giving the window length for the MA algorithm. Phenolo's processing algorithm allows deriving phenological parameters at local, continental, or global scale so that the algorithm may be applied under different climatic regions, ecosystems and land-use. Applying the MA filter in the forward direction (from the beginning to the end of the time series) results in a curve that lags behind the reference time-series whereas filtering in the backward direction creates a forward lagging curve (for a detailed explanation of the Phenolo approach is referred to Ivits *et al.*, 2012a). The season begin day (SBD) and season end day (SED) are determined for each pixel as the intersections of the reference time-series and the forward and backward lagged MA curves respectively. The distance between SBD and SED is defined as the SL (expressed in days) used as a proxy for the length of the vegetation growing season. The area under the yearly reference time-series curve, delineated by the value of the two minimums (MIN) and the yearly maximum, is the NDVI Large Integral ($NDVI_{lin}$), a proxy for vegetation productivity during the yearly growth cycle (Fig. 1b). The $NDVI_{lin}$ and SL metrics were calculated for each year between 1999 and 2010.

Bioclimatic and land cover maps

The Global Environmental Stratification (GEnS, Metzger *et al.*, 2012) was used for the analysis of bioclimatic differences in ecosystem responses to drought in the period 1999–2010. The GEnS is a consistent quantitative stratification of the land surface into relatively homogeneous bioclimatic zones supplying the current analysis with a spatial framework. The GEnS consists of 125 strata and 18 global environmental zones at a 30 arcsec resolution (equivalent to 0.86 km^2 at the equator). The environmental strata were resampled to match the spatial resolution of the remote sensing data set and were regrouped into four major bioclimatic zones (Table 1).

To assess different responses of land covers to drought, we chose the Global Land Cover 2000 database (GLC2000, Bartholome & Belward, 2005). The land cover classes were aggregated to focus the study on major European land cover types (Table 1). The class sparse vegetation, although covering substantial area, was not included in the study since for these areas the NDVI signal is subject to considerably uncertainty (Huete, 1989) influencing on the derivation of SL and $NDVI_{lin}$. The mosaic vegetation classes (including land covers as tree

Table 1 Bioclimatic zones regrouped from the GEnS and the GlC 2000 classes used in the study

Bioclimatic zones reclassified from the GEnS classes	Bioclimatic Zones
Cold and Wet (E); Extremely cold and mesic (F); Cold and mesic (G)	North/Mountains (N)
Cool temperate and dry (H); Cool temperate and xeric (I)	Continental (C)
Cool temperate and moist (J)	Temperate (T)
Warm temperate and mesic (K); Warm temperate and xeric (L); Hot and dry (N)	Mediterranean (M)
GLC 2000 classes	Abbreviation
Irrigated agriculture	Ir
Rainfed agriculture	Rf
Forests	Frst
Grasslands	Grs
Shrublands	Shrb
Wetland	Wtl

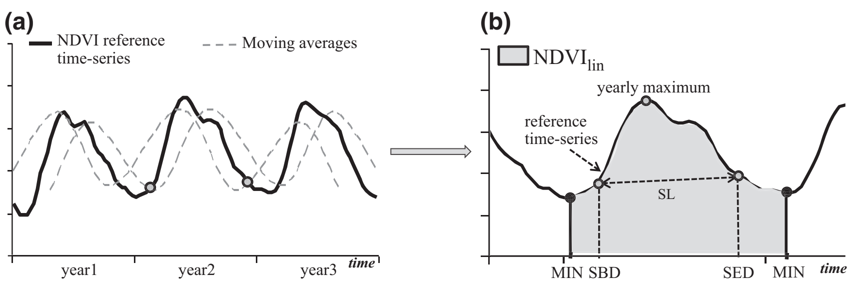

Fig. 1 Schematic representation of vegetation phenology (SL) and productivity ($NDVI_{lin}$) calculated from the NDVI time-series using moving averages.

cover, cropland, shrubland, and/or other natural vegetation to some extent) were also not considered in the present study as these classes are fragmented and widely scattered in Europe. The GLC2000 classification was also used to mask out nonvegetated areas (bare areas, water bodies, snow, ice, and artificial surfaces).

Spatio-temporal variability of drought

The spatio-temporal variability of drought between 1999 and 2010 was assessed by applying a PCA to the correlation matrix of the SPEI12 time-series. The first k PCs (i.e. eigenvectors) were selected, with k being the number of PCs that explained 90% of the total variance in the SPEI12 time-series. The time-series of the normalized PCs were analyzed to indicate the dominant temporal oscillations observed in the SPEI12 data. Spatial patterns of these temporal oscillations were calculated by correlating over each pixel the selected k PCs with the original SPEI12 time series. The per-pixel correlation maps gave a synoptic view of the strength of the relationship between the SPEI12 at the pixel level and each selected PC.

A given region might have been affected by long-term changes in precipitation and temperature conditions but also by recurrent drought events with a higher interannual variability. At European scale, this may result in complex ecosystem responses and therefore we further analyzed the correlation maps that captured dominant information of anomalies and trends at different timescales. The correlation maps were submitted to an Isodata clustering process where per-pixel correlations were spatially averaged into clusters. This generated a cluster map of Europe where pixels were classified according to the dominant precipitation and heat anomalies observed between January 1999 and December 2010 (subsequently called drought clusters or DC's). Average SPEI temporal profiles were derived for each DC and for further analysis only pixels having a significant positive correlation ($P < 0.001$) with the cluster averaged SPEI profile were considered. In this way, we focus the study on pixels where the drought conditions observed between 1999 and 2010 are similar to the dominant temporal oscillations observed in the SPEI12.

Drought footprints on ecosystem's phenology and productivity

Ecosystem phenological and productivity responses to drought were assessed using the steadiness index (Ivits *et al.*, 2012b) applied to the $NDVI_{lin}$ and SL series respectively. The steadiness index is based on convergence of evidences of positive or negative dynamics by combining two measures: (i) the slope of the linear trend defining the general, monotonous dynamic of the ecosystem phenology or productivity metrics and (ii) the net change of the metric by applying Multi-Temporal Image Differencing that provides the accumulated net interannual metric difference over a given period (Guo *et al.*, 2008). The index has four classes: Class 1 indicates strong negative dynamics of the variable (i.e. a negative net change and a negative trend) whereas class 4 indicates strong positive dynamics of the variable (a positive net change together with a positive trend). The steadiness classes 2 and 3 indicate ecosystems with generally stable phenological and productivity conditions where the system fluctuates but does not change equilibrium (Ivits *et al.*, 2012b). In the present study, we analyzed three steadiness classes: 1 representing negative change, 2 and 3 together representing no change and 4 representing positive change of the $NDVI_{lin}$ and SL time series. It must be noted, however, that transient negative events during the observation period are not captured by the steadiness index as it is based on linear trends.

The DC's, the bioclimatic zones and the land cover classes were spatially intersected to account for ecosystem response to drought events in different bioclimatic regions under various land cover classes. The negative, positive, and no change categories of the $NDVI_{lin}$ and SL steadiness classes were intersected to their nine possible combinations. Subsequently the number of pixels of the $NDVI_{lin}$ and SL combinations falling within each of the spatial entities of the DCs, bioclimatic zones and land cover classes were calculated. To analyze the spatial distribution of affected ecosystems, a Correspondence Analysis (CA) was conducted over the cross-tabulation table with the $NDVI_{lin}$ and SL combinations as columns and the spatial entities of the DCs, bioclimatic zones and land cover classes as rows. The CA was run separately for each DC and results are presented as bi-plots of the first two CA dimensions. Proximity measured in the bi-plots by Euclidean distances between the spatial entities and the steadiness classes of $NDVI_{lin}$ and SL indicates the association of the phenological and productivity dynamics of the given bioclimatic zone, DC, and land cover. Spatial entities covering less than 50 km^2 were not considered essential for the quantification of drought footprint on the ecosystems at continental scale and were therefore discarded. Spatial entities lying at the outer end of the ordination biplot represent ecosystems, DC's, land covers, and $NDVI_{lin}$/SL change dynamics covering relatively small areas (moderately bigger than 50 km^2) and having very little or no contribution to the ordination analysis.

Results

Spatio-temporal variability of drought between 1999 and 2009 in Europe

The first 12 PCA dimensions (PCs) explained 90% of the variation in the European subset of the SPEI time-series and were selected for the analysis. The 12 spatial patterns of the selected PCs, i.e. per-pixels correlation maps (Fig. S1), were submitted an Isodata clustering process resulting in four dominant clusters of drought types (DC1-4; Fig. 2a, Table 2). Averaged SPEI profiles were extracted for each of the four DC's and correlated with the original per-pixel SPEI time series (Fig. 2b). Pixels being negatively correlated with its respective cluster-averaged SPEI profile, or having a nonsignificant ($P > 0.001$) positive correlation, were not considered for further analysis. The

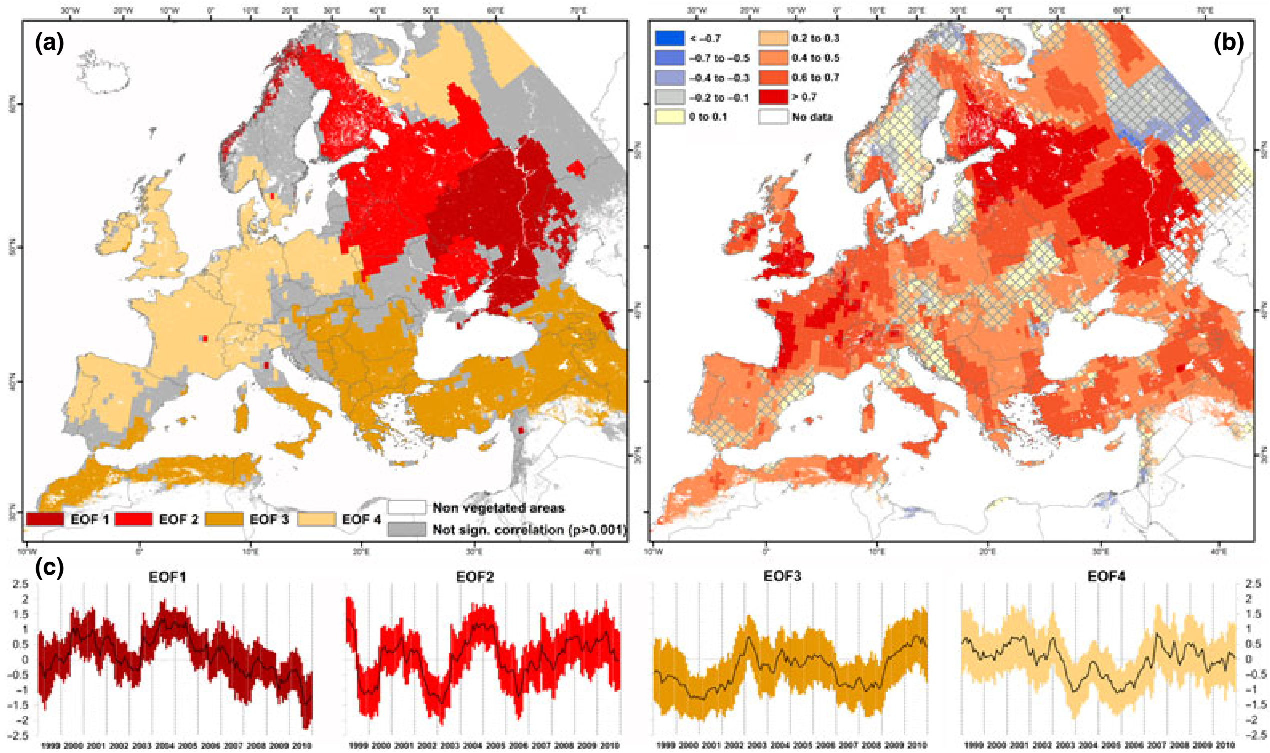

Fig. 2 (a) Drought Clusters (DC 1-4) extracted from the first 12 PCA dimensions by ISODATA clustering. (b) Correlations of the SPEI time-series to the cluster's average SPEI temporal profile. Hatched areas correspond to nonsignificant positive correlations ($P < 0.001$) or to negative correlations. White areas correspond to nonvegetated areas and were not analyzed. (c) Graphs correspond to the spatial average SPEI12 (±1 SD) for each Drought Cluster, estimated from the original monthly SPEI12 time series.

Table 2 The four drought type combinations in Europe between 1999 and 2010

Drought cluster	Short description
DC1; continental Eastern Europe	Drought events in 1999, in 2002–2003 and major drought events from 2008 on with a peak in 2010
DC2; Northern and North-East Europe	Recurrent drought events in 1999–2000, in 2002–2003, and in 2006
DC3; Continental and Mediterranean regions	Recurrent drought events between 1999 and 2002 and in 2007–2008
DC4; North Russia, Atlantic regions, Germany, Poland, Iberian Peninsula	Recurrent drought events in 2003–2004 and in 2005–2006

cluster-averaged SPEI profiles (Fig. 2c) represent the dominant temporal oscillations in drought conditions for each DC (Table 2).

The DC1 groups pixels with major drought events beginning in 2008 and reaching a peak in 2010 together with secondary drought events in 1999 and 2003 (Fig. 2c). The 2010 drought event was the strongest in Europe with an average SPEI value of −1.5. DC1 mostly covers Southern Russia reaching the North East coast of the Black Sea and the coastline of the Norwegian Sea in Scandinavia (Fig. 2a). DC2 groups pixels with recurrent drought events in 1999–2000, in 2002–2003, and in 2006 with average SPEI values of −1.4 (Fig. 2c). This drought cluster mostly covers the Northern (Finland, the Baltic States, and Russia) and the eastern Continental regions (the cost of the Black Sea in Ukraine). DC3 groups pixels with recurrent drought events in 2000–2001 and in 2007–2008, with averaged SPEI values around −1.2. This cluster is the second largest in Europe and mostly covers the Continental and Eastern Mediterranean regions (Figs 2a and 3). DC4 groups pixels with recurrent drought events in 2003–2004 and in 2005–2006. Both events had an average SPEI value of −1.1. This cluster is the largest in Europe covering Northern Russia and the Temperate Atlantic regions but also Continental (Germany and Poland) and Mediterranean (Iberian Peninsula) Europe (Figs 2a and 3).

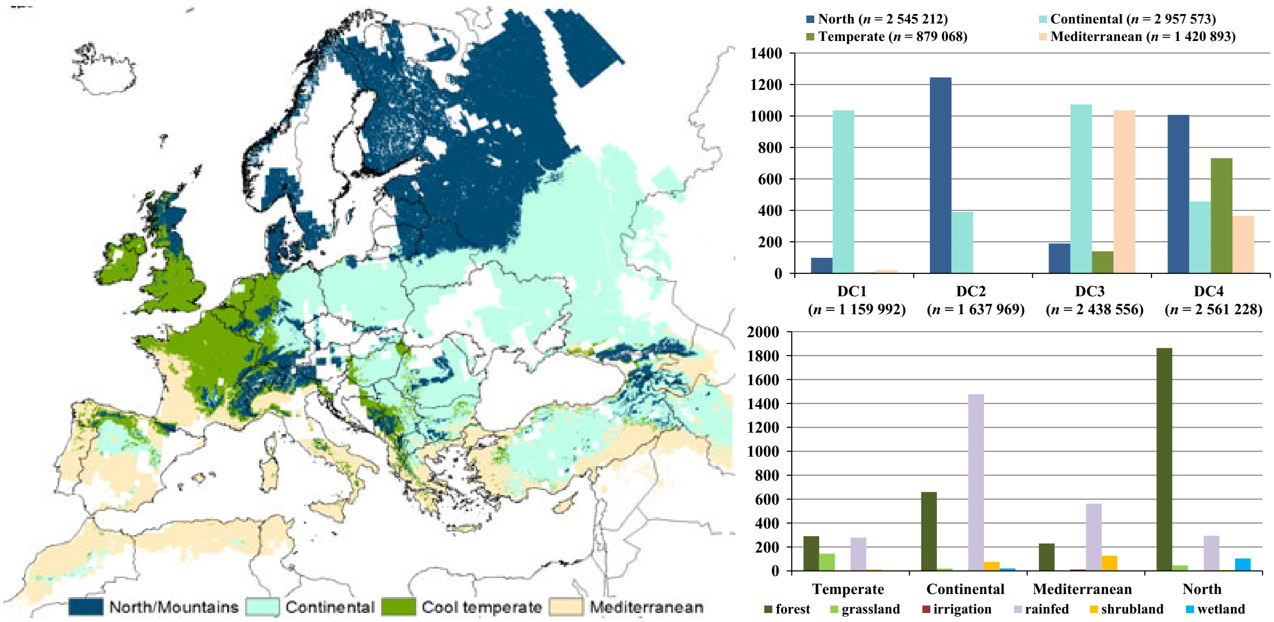

Fig. 3 Spatial distribution of the four bioclimatic zones under the drought clusters. White areas correspond to nonvegetated areas or to nonsignificant ($P < 0.001$) correlations of the SPEI time-series to the cluster's average SPEI profile (shown in Fig. 2c). Graphs show the area covered by each bioclimatic zone within each drought cluster (top right) and the area covered by each land cover within bioclimatic zone (bottom right). Areas are expressed in 1000 km^2.

Ecosystem's responses to drought between 1999 and 2010: a European overview

Despite recurrent droughts between 1999 and 2010, increased vegetation productivity was observed over most of Europe [53%; Fig. 4 – green/blue colors; change combination specific values (in% of the respective area) are shown in pie charts]. A majority of pixels with increased vegetation productivity, approximated by $NDVI_{lin}$, also presented increased SL. 20% of Europe's drought affected areas are characterized by a decrease in vegetation productivity between 1999 and 2010 (Fig. 4 – red colors). However, increased SL was observed for approximately half of the area of negative productivity dynamics (9%).

Ecosystem's responses to drought between 1999 and 2010: areas with decreased vegetation productivity

Large areas with decreased productivity and decreased or stable SL were observed over the Temperate and Continental regions, where ~15% of both regions show this development (Fig. 4). The largest agglomeration of pixels with decreased $NDVI_{lin}$ and shorter or stable SL was observed in Southern Russia where a major drought event was registered from 2008 to 2010 (DC1, Fig. 2). In the same drought cluster, decreased $NDVI_{lin}$ was observed even where SL increased (i.e. NDV_{Ilin} −SL+). Another strong agglomeration of decreased $NDVI_{lin}$ with shorter or stable SL was observed in Western France and in Germany associated with the DC4 corresponding to recurrent drought events in 2003–2004 and in 2005–2006 (Fig. 2c). Similarly to Southern Russia, large areas of decreasing or stable $NDVI_{lin}$ and increased SL (i.e. $NDVI_{lin}$−SL+ and $NDVI_{lin}$0SL+) were registered in DC4 (Fig. 4, Central and Northern Germany, Denmark and the south of UK). Smaller areas with decreased $NDVI_{lin}$ and shorter SL were also observed in Spain at the Portuguese border along the Douro river valley also associated with DC4. Finally, decreased $NDVI_{lin}$ and shorter SL were also observed over the North-Western part of Kazakhstan associated with DC2 corresponding to recurrent droughts in 1999–2000, in 2002–2003 and in 2006 (Fig. 2c).

Ecosystem's responses to drought between 1999 and 2010: areas with increased vegetation productivity

Large areas in the Northern and Mediterranean regions show increased $NDVI_{lin}$ together with increased or stable growing season (59.8% and 52.5% of the drought affected areas respectively) whereas smaller areas with increased $NDVI_{lin}$ were observed in the Continental region (21.9%). Large agglomerations of increased $NDVI_{lin}$ with longer SL ($NDVI_{lin}$+SL+) were observed in Russia and Finland despite the fact that these regions were associated with different DC's (i.e. DC2 & 4). Increased $NDVI_{lin}$ and SL observed in the

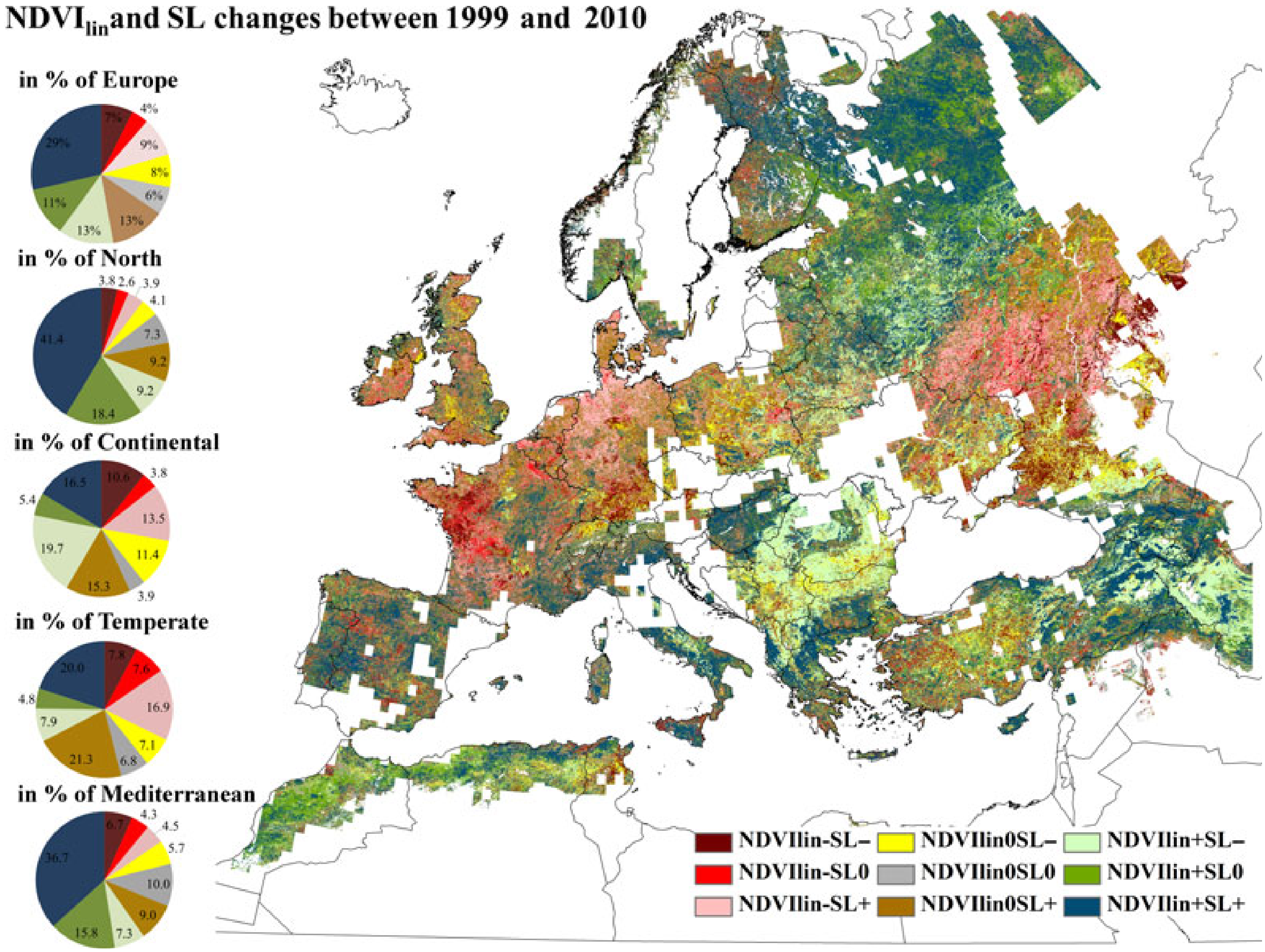

Fig. 4 Productivity ($NDVI_{lin}$) and phenological (SL) change combinations. White areas correspond to nonvegetated areas or to nonsignificant ($P > 0.001$) correlations of the SPEI time-series to the cluster's average SPEI profile. Pie charts indicate the percentage cover of each bioclimatic zone for the $NDVI_{lin}$ and SL change combinations.

Mediterranean region were associated with either DC3 (e.g. in South East Spain, Southern Italy, Albania, Greece, Hungary, and Southern Bulgaria) or with DC4 (e.g. South-East France, North Italy, and parts of Spain and Portugal). The Northern part of Bulgaria, the Southern part of Romania, the Eastern part of Serbia, and Montenegro, all areas associated with the DC4, are characterized by increased $NDVI_{lin}$ despite of shortened SL ($NDVI_{lin}$+SL−).

Effect of land covers on ecosystem's responses to drought

Figure 5 presents the results of the CA for the four drought types in Europe, showing the differences in changes in $NDVI_{lin}$ and SL per bioclimatic zones and land cover classes. The major drought event in 2008–2010 in Russia (DC1) was associated with clearly distinguishable effects on the ecosystems as a function of bioclimatic zones and land cover classes. In Fig. 5a, the first axis represents a strong gradient that separate ecosystems with increased and decreased productivity whereas the land cover classes were distinguished by diverse SL changes. Most land cover classes in the Continental regions presented the strongest correlations with the SPEI temporal profile of DC1 (cf. size of triangles in Fig. 5a) indicating drought conditions similar to the ones described by this cluster (Fig. 2c). However, the respective vegetation responses to drought varied amongst land cover classes: Rainfed agriculture (Crf) and Wetlands (Cwtl) showed a decrease in $NDVI_{lin}$ and longer growing season whereas forests (Cfrst) have increased $NDVI_{lin}$ despite shorter SL. This suggests that the impact of drought conditions was larger in rainfed agriculture and in wetlands than in forested areas. Over grasslands (Cgrs) the productivity remained stable and the SL partly decreased and partly increased (NDV_{Ilin} 0SL+ and $NDVI_{lin}$0SL−). Similar to forests but with a lower correlation to the SPEI profiles of DC1,

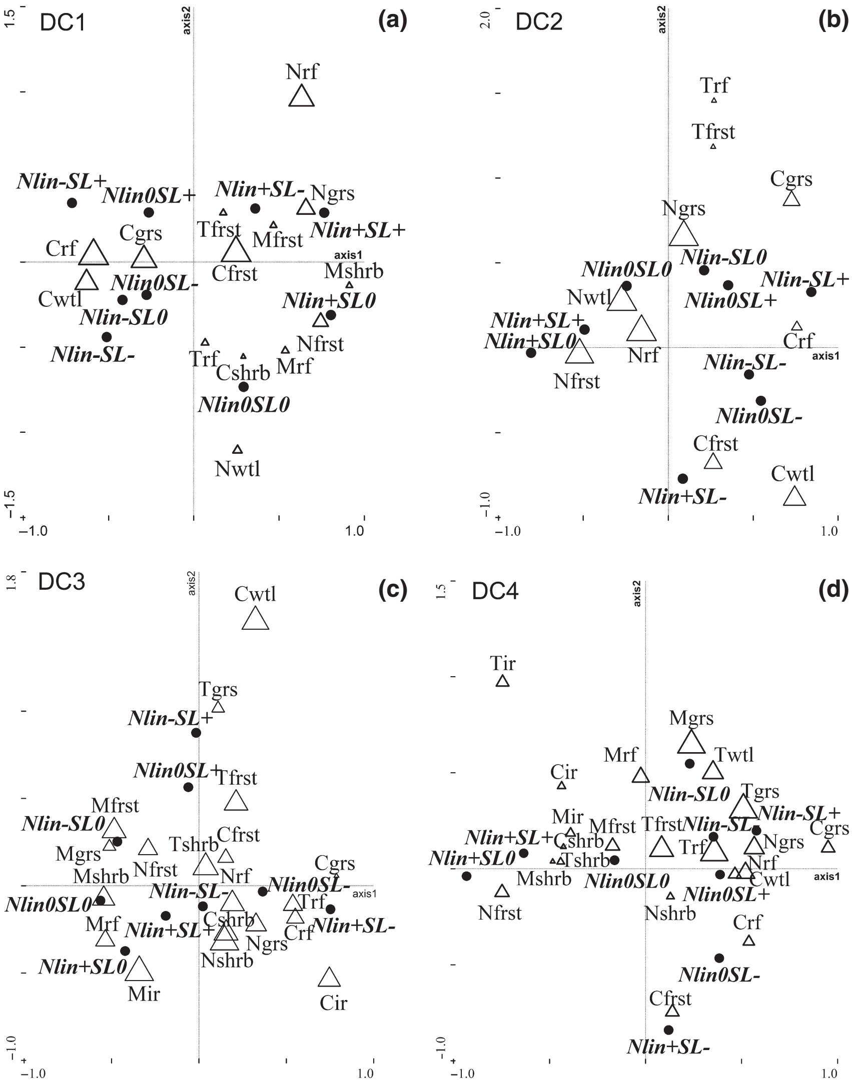

Fig. 5 Correspondence Analysis of the four major drought types in Europe where each bi-plot represents one of the drought clusters (DC1-4). Triangles represent the spatial observations of the bioclimatic zones (Northern: N, Continental: C, Temperate: T and Mediterranean: M) intersected with the land cover classes. The size of each triangle is proportional to the correlation of each spatial observation with the SPEI temporal profile of the given drought cluster. Black circles indicate the combined $NDVI_{lin}$ and SL steadiness classes (+: increase; −: decrease; 0: no change). For the abbreviations see Table 1.

shrublands (Cshrb) seemed to have buffered well the effect of drought as neither the productivity nor the SL have changed. Northern and Mediterranean land cover classes within DC1 showing increased productivity and longer growing seasons ($NDVI_{lin}$+SL+) also appear to have counteracted the drought events observed between 1999 and 2010. $NDVI_{lin}$ and SL temporal profiles for these areas also indicate the relative recovery by 2010 (Fig. 6a and d). Wetlands of the Northern ecosystems (*Nwtl*) and shrublands of the Continental region (*Cshrb*) expressed rather unchanged phenology and productivity ($NDVI_{lin}$0SL0), but the correlation with DC1 was low and the affected areas were small.

An important gradient distinguishing the bioclimatic zones by their productivity response and by their SL changes was also detected within DC2 (ranging mainly from North Russia, and Bielorussia to Finland, Fig. 2a). The Northern ecosystems showed the strongest correlations with the SPEI profiles of this cluster (Fig. 5b) but most of the land cover classes appeared to have counteracted the drought events showing increased or stable productivity and phenology. Also $NDVI_{lin}$ and SL temporal profiles for Northern regions (Fig. 6e) show a relative recovery of the affected regions as both time series indicate an upward trend. Only grasslands of the Northern regions (*Ngrs*) showed mixed responses to

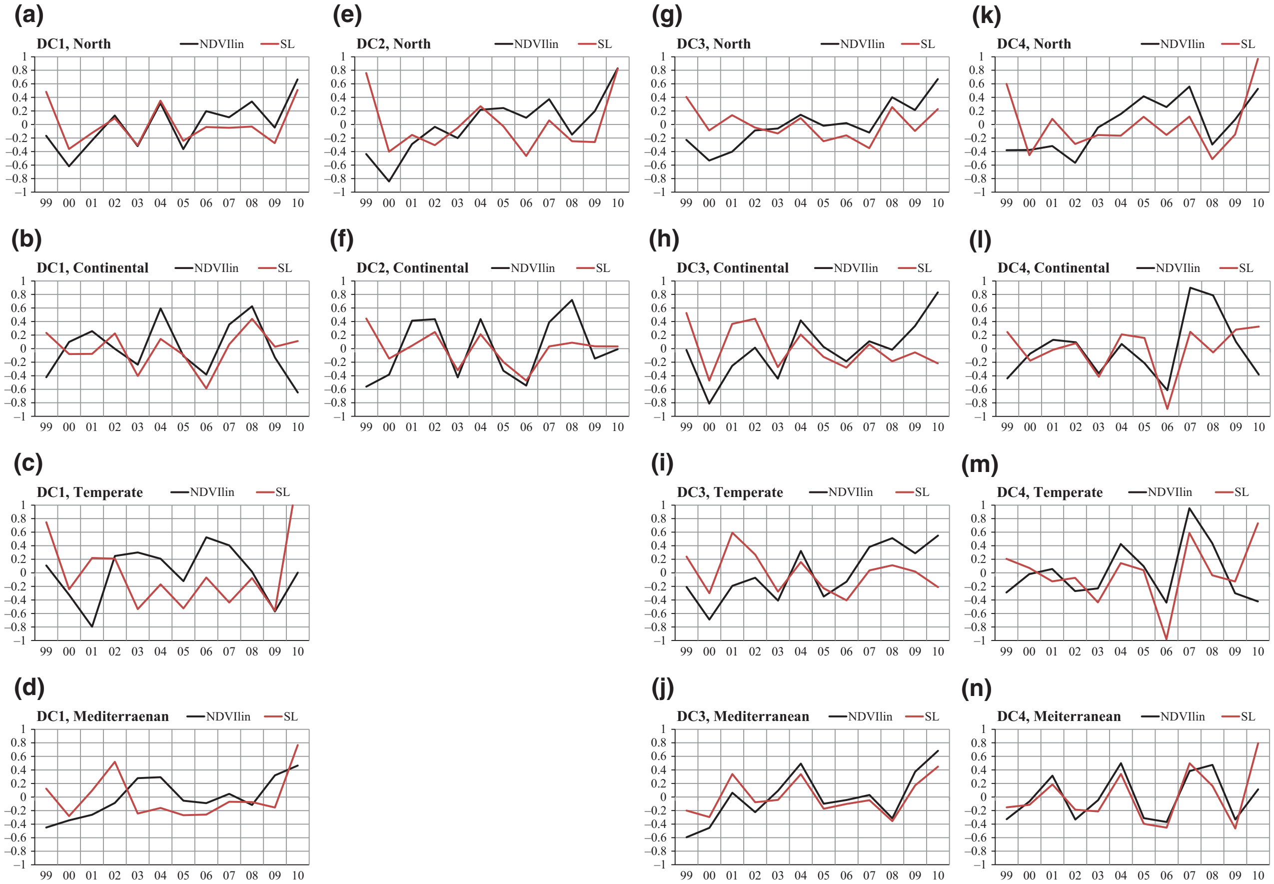

Fig. 6 Temporal profiles of the $\mathrm{NDVI_{lin}}$ and SL time-series within the four bioclimatic zones of the four drought clusters (DC 1-4). The $\mathrm{NDVI_{lin}}$ and SL values were z-score normalized with zero mean and a standard deviation = 1 to allow the comparison of the temporal records within the same scale [−1; 1]. The Temperate and Mediterranean regions of the DC2 were not analyzed due to the very small area coverage.

DC2 (plotted closer to the decreased productivity response). At the contrary, several land cover classes in the Continental region are characterized by decreased productivity (Fig. 6f) indicating that most of the Continental areas were affected with decreasing productivity and shortened seasons in 2003 and 2006 without a clear recovery. For rainfed agricultural areas (*Crf*) and grasslands (*Cgrs*) of DC2 the growing season increased but the productivity remained stable or decreased ($\mathrm{NDVI_{lin}}$0SL + and $\mathrm{NDVI_{lin}}$−SL +) whereas forests and wetlands (*Cfrst* and *Cwtl*) show increased or stable productivity despite shorter growing season ($\mathrm{NDVI_{lin}}$+SL−). No clear ecosystem responses over the Temperate and Mediterranean regions could be observed, probably due to (i) the limited number of pixels of these bioclimatic zones in DC2 and (ii) to the lower correlations observed between the original SPEI time series and the cluster averaged profiles.

In DC3 the first CA axis distinguished continental ecosystems with decreased growing season (SL−) from the Mediterranean regions with stable seasons (SL0) (Fig. 5c). The second axis differentiates vegetation response per land cover class. The recurrent droughts between 1999 and 2002 seemed to have affected vegetation development more than the 2007–2008 drought, as clear negative $\mathrm{NDVI_{lin}}$ and SL anomalies were registered in 2000 for all bioclimatic zones (Fig. 6g–j). The vegetation response to these drought events was variable depending on the land cover. In Continental and Temperate regions, stable or increasing productivity was observed in rainfed agriculture (*Crf* and *Trf*) despite the shorter growing season ($\mathrm{NDVI_{lin}}$0SL− and $\mathrm{NDVI_{lin}}$+SL−). Over grasslands and irrigated agriculture of the continental regions (*Cgrs* and *Cir*) $\mathrm{NDVI_{lin}}$ also increased but decreasing SL was observed ($\mathrm{NDVI_{lin}}$+SL−). Over rainfed and irrigated agricultural areas (*Mrf* and *Mir*) $\mathrm{NDVI_{lin}}$ increased with stable or longer seasons ($\mathrm{NDVI_{lin}}$+SL0 and $\mathrm{NDVI_{lin}}$+SL+). Forests and grasslands (*Mfrst* and *Mgrs*) on the other hand were clearly associated with decreased productivity and stable season whereas both $\mathrm{NDVI_{lin}}$ and SL remained stable ($\mathrm{NDVI_{lin}}$0SL0) in shrublands (*Mshrb*).

The DC4 associated with major drought events in 2003–2004 (most prominently in France) and 2005–2006 (most severe in Spain) showed clear regional differences: the Northern ecosystems showed recovery with increasing $NDVI_{lin}$ and SL trends whereas the Mediterranean expressed rather fluctuating vegetation development without clear upward or downwards trends (Fig. 6k and n). The Continental and Temperate regions on the other hand showed clear impacts on both productivity and SL with the peak of the negative response in 2006 (Fig. 6l and m). The CA showed that the variability in $NDVI_{lin}$ and SL changes was rather driven by land cover classes than by bioclimatic zones (Fig. 5d). Grasslands of the Continental, Temperate, and Northern regions (*Cgrs*, *Tgrs* and *Ngrs*) all showed decreased productivity despite longer growing season (NDVIlin−SL+). Grasslands of the Mediterranean (*Mgrs*) and wetlands of the Temperate (*Twtl*) regions showed a clear and strong association to decreased productivity and stable season ($NDVI_{lin}$−SL0). Rainfed agriculture exhibited rather different vegetation responses depending on the bioclimatic zone. Both in the Mediterranean (*Mrf*) and in the Temperate regions (*Trf*) productivity decreased with shorter or stable season, respectively, while in the Northern (*Nrf*) and Continental regions (*Crf*) productivity remained stable with longer or shorter growing season, respectively. Irrigated agriculture in the Continental, Mediterranean, and Temperate regions showed increased productivity and longer growing season ($NDVI_{lin}$+SL+), thereby highlighting different vegetation responses compared with rainfed agriculture. Shrublands of the Continental (*Cshrb*), Temperate (*Tshrb*), and Mediterranean (*Mshrb*) regions and forests of Northern Europe (*Nfrst*) seemed to be amongst the least affected land cover classes as they expressed increased productivity and longer or stable growing season ($NDVI_{lin}$+SL+/0).

Discussion

Drought and heat wave footprints on vegetation: dependence on bioclimatic zones and land cover

Four major drought occurrences differing in intensity, timing, duration, and location were identified over Europe for the period 1999–2010. For each of these drought events the corresponding areas being affected by recurrent drought events and heat waves were mapped. Results showed that most of Europe was exposed to drought to some extent in the period 1999–2010 with major events over the Western Atlantic regions and over North and North-Eastern Europe. The observed spatio-temporal pattern of drought only partly co-occurred with negative effects on vegetation productivity and phenology. Despite exposure to drought, increased productivity was observed in 53% of the drought affected areas and for around half of this area the length of the growing season has increased as well. Only for 20% of Europe's drought affected area a decrease in productivity was observed and only 7% of this area experienced shortened growing season as well. Thus, drought and heat wave impacts on ecosystems productivity were not apparent when assessing the net effects at continental scale. However, large regional differences were seen in the way ecosystems in diverse bioclimatic zones reacted to climatic variations with the Northern and the Mediterranean ecosystems being more resilient to drought than the Atlantic and Continental regions. In the following we discuss these predominant regional drought events and differences.

Northern ecosystems are rather subject to temperature variations than to water availability as main constraint for vegetation growth (Peñuelas *et al*., 2007). This may explain the here observed increase in productivity and growing SL (Fig. 4 pie chart) despite recurrent droughts. The positive vegetation development was mostly observed in forested ecosystems, being the main land cover of the Northern regions, but smaller not-forested ecosystems of the Northern regions also showed these trends. These results are in line with Rustad *et al*. (2001), Beier *et al*. (2004), Peñuelas *et al*. (2007) and with Zeng *et al*. (2011) reporting larger positive response of above ground plant productivity to warming climate in colder ecosystems and with Lindner *et al*. (2010) estimating increased forest productivity in northern Europe. Increased nutrient mineralization (N and/or P) and soil organic matter in warmer soils (Kirschbaum, 1995) due to warmer temperatures associated with drought periods might also have contributed to the observed productivity increases. The longer growing seasons in the Northern ecosystems might also be a direct effect of the shorter snow cover period and earlier snow melts as a result of increased minimum air temperature at the beginning of the growing season (Walther *et al*., 2002), resulting from changing climate and warming temperatures in Northern Europe (Seneviratne, 2012).

Longer growing season with increased productivity was observed also over the ***Mediterranean region*** (Fig. 4 pie chart), probably due to the stronger resilience and recovering capacity of these areas owing to their historical habituation to climatic fluctuations as reported by Larcher (2000) and Peñuelas *et al*. (2001). However, rainfed agriculture in the Iberian Peninsula showed decreased productivity and shorter growing season whereas over irrigated areas increased productivity and SL was observed. Gouveia *et al.* (2009) indicated that both arable lands and forest in Portugal registered negative anomalies in vegetation productivity during the 2004–2005 drought event, with arable lands being the most affected of the two land cover types. This difference in resilience to drought for the Mediterranean forest and arable lands was also visible in Fig. 5d, *Mfrst* being closer to stable and *Mrf* being closer to negative changes in productivity. In addition Bréda *et al.* (2006) suggested that the succession of the 2003 and 2004–2005 drought events might be one of the causes for increased tree mortality in Southern France during 2004, as the 2003 drought resulted in a large number of already weakened/stressed tree individuals.

Although the ***Temperate region*** traditionally has high yearly precipitation, the present study indicates that intensive drought periods and heat waves affected ecosystem dynamics in larger parts of this region during the last decade. Ciais *et al.* (2005) estimated that the large precipitation deficit and the extreme summer heat over Eastern and Western Europe in 2003 lead to a 30% decrease of gross primary productivity at European scale. They found a pronounced productivity decrease in agricultural areas in France, Italy, Romania, and Ukraine, in line with the pronounced negative changes in productivity observed in this study over temperate rainfed agricultural areas. Ciais *et al.* (2005) also noted that temperate deciduous beech forests showed a particularly large decrease in productivity in 2003 confirming our results for temperate forests (*Tfrst*), where we observed decreased productivity and shorter season. These results suggest that the decline in productivity could indicate a lower buffering capacity of temperate ecosystems, compared with those Mediterranean regions where the cultivation of drought tolerant species may have reduced the impact of drought (Ciais *et al.*, 2005; Peñuelas *et al.*, 2007). On the other hand, increasing growing SL might show management adaptation to drought as this region mostly covers intensively managed agricultural areas with one of the highest average annual water consumption for irrigation in Europe (Wriedt *et al.*, 2008).

In the northern part of the ***Continental region*** (North of the Black Sea) productivity decreased even over those areas where the SL expressed fluctuating dynamics or even became longer. Grasslands, rainfed agriculture, and wetlands all showed negative vegetation developments. Similar to the Temperate region, recurrent droughts over this area probably resulted in declining soil moisture and associated decline in nutrient availability (Rustad *et al.*, 2001) that affected the productivity of the ecosystems. On the other hand the increasing length of the growing season over certain areas might show management adaptation to drought and to the cultivation of drought tolerant species (Ciais *et al.*, 2005; Peñuelas *et al.*, 2007). In the southern part of the Continental region, mainly over rainfed and irrigated agriculture and grasslands (Fig. 5c, *Crf, Cir, Cgrs*), increased productivity was observed despite SL expressing fluctuating dynamics. The increased was most probably due to the cultivation of drought tolerant species (Ciais *et al.*, 2005; Peñuelas *et al.*, 2007). This is also supported by our findings, as forests and shrublands of the Continental region (*Cfrst* and *Cshrb*), that are less intensively managed, expressed decreased productivity and shorter season.

Proposed methodology for assessing drought and heat wave footprints on ecosystems: advantages and limitations

Drought intensity varies both as a function of time scale and spatial extent (Vicente-Serrano, 2006; Lloyd-Hughes, 2012), making accurate assessment of drought impact on ecosystems a challenging task (Breshears *et al.*, 2005; van der Molen *et al.*, 2011). Although the assessment of changes in extreme events such as drought and heat waves has been extensively studied (Lloyd-Hughes & Saunders, 2002; Van der Schrier *et al.*, 2006; Garcia-Herrera *et al.*, 2007; Bordi *et al.*, 2009; Lloyd-Hughes, 2012; Dai *et al.* 2010; Sousa *et al.*, 2011; Gouveia *et al.*, 2012), only few studies have conducted a continental scale analysis of the effect of recurrent droughts on vegetation functioning in diverse ecosystems covering diverse bioclimatic zones (Lindner *et al.*, 2010; Sheffield *et al.*, 2012; Chen *et al.*, 2013; Vicente-Serrano *et al.*, 2013). In this study, we have presented an approach to link spatio-temporal patterns of recurrent drought events to vegetation productivity and phenological changes in Europe. Based on PCA, the methodology enables a contemporary assessment of ecosystem productivity and growing SL being affected by successive, recurrent droughts during the period of analysis. The method is easily applicable to longer time-series and to diverse spatial scales and with increasing length of the time series ecosystem resilience, recovery, or strong negative effects can be repeatedly assessed. It must be noted, that NPP is the net flux of carbon to plants from the atmosphere in unit time and defines a balance between gross photosynthesis and autotrophic respiration. Although NDVI is traditionally used in the literature to quantify absolute amounts of primary production, it has also been shown to be only a measure of photosynthetic potential (Runyon *et al.*, 1994) and it only yields estimates of relative vegetation amounts (Seaquist *et al.*, 2003). Future research should concentrate on effects of drought on a more precisely assessed NPP than the approximated value given by NDVI.

The notion of major drought events at the scale of the drought clusters (DC1-4) must be also handled with caution: mapping the correlation of pixels to the cluster-averaged SPEI temporal profiles shows the joint intensity of heat waves and precipitation shortages that has to be understood at the continental scale and does not necessarily reflect accurately the magnitude or timing of the drought events at the national/sub-national scale. For example the here presented weaker intensity drought of the Iberian Peninsula embedded in DC4 (compared with the stronger droughts captured by DC1-2, Fig. 2c) does not duly represent the worst drought episode of 2004/05 of the Iberian area being recorded in the last six decades (Garcia-Herrera *et al.*, 2007). Furthermore, the increase of $NDVI_{lin}$ in areas with a decrease of SL might not only reflect changes in precipitation and/or temperature patterns but they may also reflect important changes in land management or land cover types. In addition, this study did not assess drought effects in sparsely vegetated areas despite the fact that these ecosystems are highly sensitive to changes in precipitation. Indeed, due to the sparse vegetation cover in these areas the NDVI is subject to uncertainty due to soil background contamination. This, and possible effects of land management, can however only be answered with additional information measured on the ground and future studies should concentrate addressing these issues to accurately assess the effect of droughts on these ecosystems.

The 12-year SPOT VEGETATION time series used for vegetation change analysis as a response to precipitation shortages and heat waves in Europe does not supply any guarantee for an association to climate change nor that the observed patterns will continue. The current approach, though not appropriate to address long-term climate change impacts, is suitable to map short to medium-term ecosystem and land cover responses to extreme climate events at the regional/continental scale. It allows the identification of drought-type clusters with specific drought/heat-waves spatio-temporal patterns and groups ecosystems and/or land covers that have undergone similar drought related stresses over a relatively short period of time (here 12 years). It has a potential for providing information about the extent, severity, and frequency of extreme events. In that sense, it brings insight on the current drought resilience and recovering capacity of land covers belonging to different ecosystems and therefore could serve improving scenarios of ecosystems responses to climate changes.

Acknowledgements

This research was partly funded by the Danish Council for Independent Research (DFF) Sapere Aude programme; project entitled "Earth Observation based Vegetation productivity and Land Degradation Trends in Global Drylands". We would like to thank the Instituto Pirenaico de Ecología — CSIC and Sergio Vincent-Serrano for providing us the new SPEI time-series for the time and spatial frame of the present study. Furthermore, we acknowledge the freely downloadable SPOT Vegetation products of VITO (http://free.vgt.vito.be/).

References

Allen RG, Pereira LS, Raes D *et al.* (1998) Crop evapotranspiration: guidelines for computing crop water requirements. FAO Irrigation and Drainage Paper No 56. Food and Agriculture Organisation, Land and Water, Rome, Italy.

Anderegg WRL, Kane JM, Anderegg LDL (2013) Consequences of widespread tree mortality triggered by drought and temperature stress. *Nature Climate Change*, **3**, 30–36. doi:10.1038/nclimate1635.

Bartholome EM, Belward AS (2005) GLC2000; a new approach to global land cover mapping from Earth Observation data. *International Journal of Remote Sensing*, **26**, 1959–1977.

Beier C, Emmett B, Gundersen P *et al.* (2004) Novel Approaches to Study Climate Change Effects on Terrestrial Ecosystems in the Field-Drought and Passive Night Time Warming. *Ecosystem*, **7**, 583–597.

Bordi I, Sutera A (2001) Fifty years of precipitation: some spatially remote teleconnections. *Water Resources Management*, **15**, 247–280.

Bordi I, Fraedrich K, Sutera A (2009) Observed drought and wetness trends in Europe: an update. *Hydrology and Earth System Sciences*, **13**, 1519–1530.

Bréda N, Hucb R, Graniera A *et al.* (2006) Temperate forest trees and stands under severe drought: a review of ecophysiological responses, adaptation processes and long-term consequences. *Annals of Forest Science*, **63**, 625–644.

Breshears DD, Cobb NS, Rich PM *et al.* (2005) Regional vegetation due-off in response to global-change-type drought. *Proceedings of the National Academy of Sciences*, **102**, 15144–15148.

Brown ME, Funk CC (2008) Food security under climate change. *Science*, **319**, 580–581.

Caccamo G, Chisholm LA, Bradstock RA *et al.* (2011) Assessing the sensitivity of MODIS to monitor drought in high biomass ecosystems. *Remote Sensing of Environment*, **115**, 2626–2639.

Chen T, van der Werf GR, de Jeu RAM *et al.* (2013) A global analysis of the impact of drought on net primary productivity. *Hydrology and Earth System Sciences Discussions*, **10**, 2429–2451. doi:10.5194/hessd-10-2429-2013.

Ciais Ph, Reichstein M, Viovy N *et al.* (2005) Europe-wide reduction in primary productivity caused by the heat and drought in 2003. *Nature*, **437**, 529–533.

Dai A (2011) Drought under global warming: a review. *Wiley Interdisciplinary Reviews: Climate Change*, **2**, 45–65.

Dai A, Trenbert KE, Qian TT (2004) A global dataset of Palmer Drought Severity Index for 1870–2002: relationship with soil moisture and effects of surface warming. *Journal of Hydrometeorology*, **5**, 1117–1130.

EMDAT (2011). *The OFDA/CRED International Disaster Database*. Université Catholique de Louvain, Brussels, Belgium. Available at: www.emdat.be.

Fensholt R, Huber GS, Proud SR *et al.* (2010) Detecting canopy water status using shortwave infrared reflectance data from polar orbiting and geostationary platforms. *IEEE Journal of Selected Topics in Applied Earth Observations and Remote Sensing*, **3**, 271–285.

Garcia-Herrera R, Paredes D, Trigo RM *et al.* (2007) The outstanding 2004–2005 drought in the Iberian Peninsula: the associated atmospheric circulation. *Journal of Hydrometeorology*, **8**, 483–498.

Gouveia C, Trigo RM, DaCamara CC (2009) Drought and vegetation stress monitoring in Portugal using satellite data. *Natural Hazards and Earth Systems Sciences*, **9**, 185–195. doi:10.5194/nhess-9-185-2009.

Gouveia CM, Bastos A, Trigo RM *et al.* (2012) Drought impacts on vegetation in the pre- and post-fire events over Iberian Peninsula. *Natural Hazards and Earth Systems Sciences*, **12**, 3123–3137. doi:10.5194/nhess-12-3123-2012.

Guo WQ, Yang TB, Dai JG *et al.* (2008) Vegetation cover changes and their relationship to climate variation in the source region of the Yellow River, China, 1990–2000. *International Journal of Remote Sensing*, **29**, 2085–2103.

Horion S, Carrão H, Singleton A *et al*. (2012). *JRC Experience on the Development of Drought Information Systems. Europe, Africa and Latin America*. EUR 25235 EN. Publications Office of the European Union, Luxembourg. JRC68769, doi: 10.2788/15724. Available at: http://publications.jrc.ec.europa.eu/repository/bitstream/111111111/23582/1/lbna25235enn.pdf.

Huete AR (1989) Soil influences in remotely sensed vegetation canopy spectra. In: *Theory and Application of Optical Remote Sensing* (ed. Asrar G), pp. 107–141. Wiley, New York.

Ivits E, Cherlet M, Mehl W *et al*. (2012a) Ecosystem Functional Units characterized by satellite observed phenology and productivity gradients: a case study for Europe. *Ecological Indicators*, **27**, 17–28. doi:10.1016/j.ecolind.2012.11.010.

Ivits E, Cherlet M, Sommer S *et al*. (2012b) Addressing the complexity in non-linear evolution of vegetation phenological change with time-series of remote sensing images. *Ecological Indicators*, **26**, 49–60. doi:10.1016/j.ecolind.2012.10.012.

Ji L, Peters A (2003) Assessing vegetation response to drought in the northern Great Plains using vegetation and drought indices. *Remote Sensing of Environment*, **87**, 85–98.

Kirschbaum MU (1995) The temperature dependence of soil organic matter decomposition, and the effect of global warming on soil organic C storage. *Soil Biology and Biochemistry*, **27**, 753–760.

Landsberg HE (1986) Potentialities and limitations of conventional climatological data for desertification monitoring and control. *Climate Change*, **9**, 123–128.

Larcher W (2000) Temperature stress and survival ability of Mediterranean sclerophyllous plants. *Plant Biosystems*, **134**, 279–295.

Lindner M, Maroschek M, Netherer S *et al*. (2010) Climate change impacts, adaptive capacity, and vulnerability of European forest ecosystems. *Forest Ecology and Management*, **259**, 698–709.

Lloyd-Hughes B (2012) A spatio-temporal structure-based approach to drought characterisation. *International Journal of Climatology*, **32**, 406–418.

Lloyd-Hughes B, Saunders MA (2002) A drought climatology for Europe. *International Journal of Climatology*, **22**, 1571–1592.

McKee TB, Doesken NJ, Kliest J (1993) The relationship of drought frequency and duration to time scales. In Proceedings of the 8th Conference of Applied Climatology, Anaheim, 17-22 January, Anaheim, CA. *American Meteorology Society*, Boston, MA. 179–184.

Medlyn BE (2011) Comment on "Drought-induced Reduction in Global Terrestrial Net Primary Production from 2000 through 2009". *Science*, **333**, 1093.

Metzger MJ, Bunce RGH, Jongman RHG *et al*. (2012) A high-resolution bioclimate map of the world: a unifying framework for global biodiversity research and monitoring. *Global Ecology and Biogeography*, **22**, 630–638.

Mishra AK, Singh VP (2010) A review on drought concepts. *Journal of Hydrology*, **391**, 202–216.

van der Molen MK, Dolman AJ, Ciais P *et al*. (2011) Drought and ecosystem carbon cycling. *Agricultural and Forest Meteorology*, **151**, 765–773.

Palmer WC (1965) Meteorological drought. Res. Paper No. 45, 58pp, Dept. of Commerce, Washington, D.C.

Peñuelas J, Lloret F, Montoya R (2001) Drought effects on mediterranean vegetation and taxa evolutionary history. *Forest Science*, **47**, 214–218.

Peñuelas J, Gordon C, Llorens L *et al*. (2004) Non-intrusive field experiments show different plant responses to warming and drought among sites, seasons and species in a North-South European gradient. *Ecosystems*, **7**, 598–612.

Peñuelas J, Prieto P, Beier C *et al*. (2007) Response of plant species-richness and primary productivity in shrubland along a north-south gradient in Europe to seven years of experimental warming and drought: reductions in primary productivity in the heat and drought of 2003. *Global Change Biology*, **13**, 2563–2581.

Rhee J, Im J, Carbone GJ (2010) Monitoring agricultural drought for arid and humid regions using multi-sensor remote sensing data. *Remote Sensing of Environment*, **114**, 2875–2887.

Runyon J, Waring RH, Goward SN, Welles JM (1994) Environmental limits on net primary production and light-use efficiency across the Oregon transect. *Ecological Applications*, **4**, 226–237.

Rustad LE, Campbell JL, Marion GM *et al*. (2001) A meta-analysis of the response of soil respiration, net nirogen mineralization, and aboveground plant growth to experimental ecosystem warming. *Oecologia*, **126**, 543–562.

Samanta A, Costa MH, Nunes EL *et al*. (2011) Comment on "Drought-induced Reduction in Global Terrestrial Net Primary Production from 2000 through 2009". *Science*, **333**, 1093.

Seaquist JW, Olsson L, Ardö J (2003) A remote sensing-based primary production model for grassland biomes. *Ecological Modelling*, **169**, 131–155.

Seneviratne SI (2012) Climate science: historical drought trends revisited. *Nature*, **491**, 338–339.

Sheffield J, Wood EF, Roderick ML (2012) Little change in global drought over the past 60 years. *Nature*, **491**, 435–438.

Sousa PM, Trigo RM, Aizpurua P *et al*. (2011) Trends and extremes of drought indices throughout the 20th century in the Mediterranean. *Natural Hazards and Earth Systems Sciences*, **11**, 33–51. doi:10.5194/nhess-11-33-2011, 2011.

Udelhoven T, Stellmes M, del Barrio G *et al*. (2009) Assessment of rainfall and NDVI anomalies in Spain (1989–1999) using distributed lag models. *International Journal of Remote Sensing*, **30**, 1961–1976.

Van der Schrier GK, Briffa R, Jones PD *et al*. (2006) Summer moisture variability across Europe. *Journal of Climate*, **19**, 2818–2834.

Vicente-Serrano SM (2006) Differences in spatial patterns of drought on different time scales: an analysis of the Iberian Peninsula. *Water Resources Management*, **20**, 37–60. doi: 10.1007/s11269-006-2974-8

Vicente-Serrano SM (2007) Evaluating the Impact of drought using Remote Sensing in a Mediterranean, semi-arid region. *Natural Hazards*, **40**, 173–208.

Vicente-Serrano SM, Beguería S, López-Moreno JI (2010) A Multi-scalar drought index sensitive to global warming: the Standardized Precipitation Evapotranspiration Index – SPEI. *Journal of Climate*, **23**, 1696–1718.

Vicente-Serrano SM, Gouveia C, Camarero JJ *et al*. (2013) Response of vegetation to drought time-scales across global land biomes. *Proceedings of the National Academy of Sciences*, **110**, 52–57.

Walther GR, Post E, Convey P *et al*. (2002) Ecological responses to recent climate change. *Nature*, **416**, 389–395. doi:10.1038/416389a.

Wang J, Rich PM, Price KP (2003) Temporal responses of NDVI to precipitation and temperature in the central Great Plains, USA. *International Journal of Remote Sensing*, **24**, 2345–2364.

Wilhite DA (2000) Drought as a natural hazard: concepts and definitions. In: *Drought: A Global Assessment* (ed. Wilhite DA), pp. 3–18. Routledge Publishers, London.

Wilhite DA (2002) Combating drought through preparedness. *Natural Resources Forum*, **26**, 275–285.

WMO (2006). Drought monitoring and early warning: concepts, progress and future challenges, WMO No. 1006, WMO, Geneva.

Wriedt G, Van der Welde M, Aloe A *et al*. (2008) Water requirements for irrigation in the European Union. EUR - Scientific and Technical Research Reports, EUR 23453 EN, Geneva, Switzerland

Zeng H, Jia G, Howard EH (2011) Recent changes in phenology over the northern high latitudes detected from multi-satellite data. *Environmental Research Letters*, **6**, 045508.

Zhao M, Running SW (2010) Drought-induced reduction in global terrestrial net primary production from 2000 through 2009. *Science*, **329**, 940–943.

Supporting Information

Additional Supporting Information may be found in the online version of this article:

Figure S1. Correlation maps of the SPEI time series with the Principal Components for the first 12 dimensions.